



OPEN Improving lower-extremity artery depiction and diagnostic confidence using dual-energy technique and popliteal artery monitoring in dual-low dose CT angiography

Wancui Mei^{1,5}, Qian Tang^{2,5}, Chengcheng Li³, Sai Wang¹, Qiqi Zhou¹, Lin Xu¹, Suping Chen⁴, Chao Liu¹✉ & Wen Chen¹✉

To assess the utility of dual-energy CT scanning (DECTs) with popliteal artery (PA) monitoring in dual low-dose (radiation and contrast) lower-extremity CT angiography (LE-CTA). 135 patients undergoing LE-CTA were prospectively included and divided into three groups of 45 each. Group-A: conventional scanning, 105 mL of contrast, abdominal aorta monitoring; Group-B: low-dose DECTs, 95 mL of contrast, AA monitoring; Group-C: low-dose DECTs, 85 mL of contrast, PA monitoring. Signal-to-noise ratio (SNR) and contrast-to-noise ratio (CNR), as well as their elevations at seven arteries, were evaluated. Two radiologists conducted subjective assessments of overall image quality and vascular diagnosis in three arterial segments. They also recorded the visible branch grading in the lower-knee segment (LKS). Group-C reduced contrast and effective doses by 19.04% and 12.62%, respectively, compared to Group-A ($P < 0.001$). Group-C had the best SNR and CNR for four LKS arteries. Regarding SNR and CNR elevations, Group-C outperformed Group-B in distal arteries beyond the PA. In the LKS, Group-C performed best for subjective overall image quality, visible branch grading, and diagnostic confidence, as well as the inter-observer diagnostic consistency, followed by Group-B and Group-A ($P < 0.001$). DECTs with PA monitoring provides excellent depiction of lower-extremity arteries under dual low-dose conditions.

Keywords Dual energy CT, Lower extremity arteries, Radiation dose, Iodine contrast, Computed tomography angiography

Abbreviations

AIS	Abdominal iliac segment
ASIR-V	Adaptive statistical iterative reconstruction
AA	Abdominal aorta
ATA	Anterior tibial artery
DPA	Dorsalis pedis artery
CM	Contrast medium
CNR	Contrast-to-noise ratio
CTA	CT angiography
CTDIvol	CT Volumetric Dose Index

¹Department of Radiology, Taihe Hospital, Hubei University of Medicine, No. 32, Renmin South Rd, Maojian District, Shiyan 442000, Hubei, People's Republic of China. ²Department of Radiology, Minda Hospital, Hubei Minzu University, Enshi, People's Republic of China. ³Department of Ultrasound, Taihe Hospital, Hubei University of Medicine, Shiyan, People's Republic of China. ⁴GE Healthcare, Computed Tomography Research Center, Beijing 100176, People's Republic of China. ⁵Wancui Mei and Qian Tang have contributed equally to this work and share the first authorship. ✉email: 541238658@qq.com; taiheren007@163.com

CFA	Common femoral artery
DECTs	Dual-energy CT scanning
DLP	Dose length product
FA	Fibular artery
FPS	Femoral popliteal segment
LKS	Lower knee segment
PA	Popliteal artery
PTA	Posterior tibial artery
ROI	Region-of-interest
SD	Standard deviation
SNR	Signal-to-noise ratio

Peripheral artery disease (PAD) is a type of atherosclerosis affecting lower extremity arteries^{1,2}, leading to chronic obstruction and impacting over 200 million individuals globally^{3,4}. Lower extremity CT angiography (LE-CTA) is a noninvasive, rapid, and accurate imaging modality increasingly advocated for the assessing and diagnosing vascular diseases^{5–8}. However, the extensive anatomical distribution of lower extremity arteries often results in higher radiation exposure and increased contrast media dosage, raising concerns regarding radiation risk and potential contrast-induced adverse effects. Furthermore, the small lumen diameter of below-knee arteries and distal vascular resistance often result in inadequate or absent visualization of these vessels in conventional CT scanning. Therefore, obtaining high-quality LE-CTA of below-knee arteries maintaining a dual-low dose (contrast and radiation) remains a formidable challenge.

Recently, a variety of techniques have been employed in LE-CTA, including dual-energy CT scanning (DECTs)^{9,10}, advanced image reconstruction algorithms¹¹, and time-resolved CT sequences^{12,13}. A notable advancement is DECTs technology, which generates virtual monoenergetic images (VMIs) at varying kiloelectron voltages (keV)^{14–16}. Utilizing lower keV settings can significantly enhance iodine contrast, thus improving the visualization of lower extremity arteries^{9,15}. Furthermore, DECTs has demonstrated the capability to maintain vascular display quality with slightly reduced radiation doses and reduced contrast media doses in LE-CTA, respectively^{9,17}. However, its potential application within a dual-low dose LE-CTA protocol is yet to be further investigated.

In clinical practice, variations in individual circulation conditions complicate the routine threshold-triggering scanning mode, typically monitored at the abdominal aorta (AA). This approach often results in optimal visualization of above-knee arteries while providing suboptimal imaging of below-knee arteries, a limitation that persists even with DECTs. Previous reports have indicated that employing a popliteal artery (PA) monitoring strategy, triggered in a feet-to-head LE-CTA scanning, enhances imaging of below-knee arteries, albeit potentially with reduced efficacy for above-knee vessels¹⁸. In our preliminary experiments, PA monitoring during head-to-feet scanning also improved the visualization of below-knee vasculature; however, this methodology remains underexplored in the existing literature. Collectively, we hypothesize that the combination of DECTs and PA monitoring with a head-to-feet scanning direction may yield effective depiction of both above-knee and below-knee arteries under dual-low dose conditions.

This study aims to evaluate the clinical utility of combining DECTs and PA monitoring in enhancing the visualization of the entire lower extremity arterial system, from the abdominal aorta to the plantar arteries, and in improving diagnostic confidence within the context of dual-low dose protocols.

Materials and methods

Patient population

This prospective study was approved by the Ethics Review Committee of Taihe Hospital, Shiyan City (IRB: 2024KS81), and all patients in the study have signed written informed consent. The research involved in this study was conducted in accordance with relevant guidelines and regulations, and the declaration of Helsinki. We prospectively enrolled patients suspected of peripheral artery disease who needed lower extremity artery CTA at Taihe Hospital from September 2022 to September 2023. Inclusion Criteria: (1) age > 18 years and able to cooperate with the examination; (2) no absolute contraindications to contrast enhancement. Patients were assigned to three groups using simple randomization. Group A: conventional scanning with abdominal aorta (AA) monitoring; Group B: low-radiation-dose DECTs with AA monitoring; Group C: dual-low-dose DECTs with PA monitoring. Exclusion criteria: (1) incomplete clinical data; (2) severe motion artifacts; (3) metal artifacts.

Scanning protocol

All patients were scanned using a GE HealthCare 256-row Revolution CT scanner. (1) Position: patients were placed in a supine position with both arms raised above the head, utilizing a foot-first position, and centered on the scanning table. The scan range extended from the lower margin of the 12th vertebra to the toes. (2) Scanning parameters: Group A: a tube voltage of 100 kVp, with tube current automatically modulated between 250 and 600 mA, a noise index (NI) of 7, rotation speed of 0.7 s and a pitch of 0.98:1; Groups B and C utilized gemstone spectral imaging (GSI) mode, with the tube voltage switching rapidly between 80 and 140 kVp, with a tube current of 200 mA, a gantry rotation time of 0.5 s, and a pitch of 0.98:1; image reconstruction for all groups used an 80% adaptive statistical iterative reconstruction algorithm. (3) Technical parameters: the monitoring ROIs for Groups A and B were set at the level of the 3rd lumbar vertebra in the abdominal aorta, while the monitoring ROI for Group C was set at the popliteal artery at the knee joint. The triggering threshold for all three groups was 150 HU; after the contrast agent was injected, scanning began with an 8-s delay once the CT value in the ROI reached this threshold. (4) Contrast agent injection protocol: all patients received a non-ionic water-soluble

iodine contrast agent (Iohexol, 350 mg/mL, Omnipaque), injected via a 20-gauge intravenous catheter in the right median cubital vein. The contrast agent and saline were injected at a rate of 4 mL/s, with Group A receiving 105 mL of contrast agent followed by 45 mL of saline; Group B receiving 95 mL of contrast agent followed by 55 mL of saline; and Group C receiving 85 mL of contrast agent followed by 65 mL of saline.

Image post processing

After the examination, all images were transferred to the AW 4.7 image post-processing workstation (GE HealthCare), where Groups B and C had 50 keV monochromatic images generated. All images underwent maximum intensity projection (MIP) and volume rendering (VR) post-processing techniques.

Objective measurements

Two radiologists, respectively with over 5 (reader 1) and 10 (reader 2) years of experience in vascular diagnostics, measured the CT values and noise values (SD) of the AA, common femoral artery (CFA), PA, anterior tibial artery (ATA), posterior tibial artery (PTA), fibular artery (FA), and dorsalis pedis artery (DPA) three times consecutively at adjacent slices, taking the average value as final. The circled ROI was selected near the center of the vessel, with the area close to the lumen while avoiding vessel walls or calcified plaques. In cases of complete vessel occlusion, measurements were taken from adjacent vessels. The SD value of the psoas major muscle at the same level as the AA was measured as background noise, with an ROI size of approximately 20 mm², and the average value was recorded. The signal-to-noise ratio (SNR) and contrast-to-noise ratio (CNR) for the three groups were calculated, as well as the elevation rates of SNR and CNR for Groups B and C compared to Group A, and Group C compared to Group B. The calculations followed listed equations:

- (1) $SNR = CT \text{ value}_{\text{target vessel}} / SD_{\text{target vessel}}$;
- (2) $CNR = (CT \text{ value}_{\text{target vessel}} - CT \text{ value}_{\text{muscle}}) / SD_{\text{muscle}}$;
- (3) $SNR \text{ elevation}_{B \text{ or } C \text{ to } A} (\%) = [(SNR_{B \text{ or } C} - SNR_A) / SNR_A] \times 100\%$;
- (4) $CNR \text{ elevation}_{B \text{ or } C \text{ to } A} (\%) = [(CNR_{B \text{ or } C} - CNR_A) / CNR_A] \times 100\%$;
- (5) $SNR \text{ elevation}_{C \text{ to } B} (\%) = [(SNR_C - SNR_B) / SNR_B] \times 100\%$;
- (6) $CNR \text{ elevation}_{C \text{ to } B} (\%) = [(CNR_C - CNR_B) / CNR_B] \times 100\%$.

Subjective image evaluation

All images were assessed by two radiologists respectively with 5 (reader 1) and over 10 years (reader 2) of experience in vascular diagnostics, respectively, without knowledge of group or patient information. The entire lower-extremity arteries were divided into three segments: Abdominal Iliac Segment (AIS, including the abdominal aorta, common iliac artery, and external iliac artery); Femoral Popliteal Segment (FPS, including the common femoral artery, deep femoral artery, superficial femoral artery, and popliteal artery); and Lower Knee Segment (LKS, including the tibiofibular trunk, anterior tibial artery, posterior tibial artery, fibular artery, and dorsalis pedis artery). Overall image quality was evaluated in the three segments, while the visible branch grading was assessed only for the LKS. A 5-point scale was used to evaluate overall image quality based on noise, artifacts, sharpness, and vascular visibility¹⁹. The scoring criteria were as follows: 5 points (excellent)—minimal noise and artifacts, clear vessel contours, excellent image quality; 4 points (good)—low noise or artifacts; clear vessel contours, good image quality; 3 points (fair)—mild noise or artifacts; partially blurred vessel contours, average image quality; 2 (poor)—high noise or heavy artifacts; unclear vessel contours, poor image quality; 1 (unacceptable)—severe noise and artifacts, unacceptable image quality. Scores of 3 or above were considered as meeting the diagnostic requirement. The below-knee arteries were graded based on the origin of arterial branches, with the furthest visible arterial branch recorded: Grade 1 for visible popliteal artery; Grade 2 for visible anterior and posterior tibial arteries; Grade 3 for visible small arteries branching from the anterior and posterior tibial arteries and fibular artery; Grade 4 for visible branches of Grade 3 arteries and the dorsalis pedis artery; Grade 5 for visible small branches and abundant plantar arteries. The highest grade was recorded.

Diagnostic performance

Two radiologists with different levels of experience (the senior with 20 years called reader 3 and the junior with 5 years in vascular diagnostics called reader 4) conducted diagnostic evaluations without knowledge of group assignment or clinical information. Diagnosis was based on LE-CTA guidelines²⁰, assessing lesions such as vascular calcification, stenosis, and occlusion. The scoring criteria were as follows: 5 points for definite presence of lesions, 4 points for possible presence of lesions, 3 points for uncertainty, 2 points for possible absence of lesions, and 1 point for definite absence of lesions. A score of 3 or higher indicated a diagnosis of lesion presence, while a score below 3 indicated absence. Strong diagnostic confidence was indicated by scores of 5 or 4 (3 points), moderate confidence by scores of 4 or 3 (2 points), and poor confidence by a score of 3 (1 point).

Radiation dose

The CT volumetric dose index (CTDI_{vol}, mGy) and dose-length product (DLP, mGy·cm) were recorded from the dose reports generated after CT scans. The effective radiation dose (ED, mSv) for each patient was calculated using the formula $ED = DLP \times K$, where K for males is 0.0056 and for females is 0.0068²¹.

Statistical analysis

Data management and statistical analysis were performed using SPSS 27.0. Sample size calculations were conducted with PASS software (NCSS, East Kaysville, UT, USA), with a statistical power at 0.9. Power calculations assumed data analysis would use Welch's test with a significance level of 0.05. Based on the preliminary experimental results of this study, we set the means and standard deviations for the three groups as 13.35, 14.36, 18.6 and 4.57, 5.35, 7.23, respectively. PASS calculations indicated that a minimum of 105 subjects with 35 cases per group was required. Accounting for a 10% dropout rate, a total of 117 individuals should be enrolled. Categorical variables (e.g., gender, age, underlying disease) were represented as numbers and compared using chi-square tests or Fisher's exact test. Continuous variables were expressed as mean \pm standard deviation, while subjective scores were presented as median (minimum, maximum)²² and compared using the Kruskal–Wallis H test. The consistency of subjective scores between the two radiologists was evaluated using Kappa statistics, where Kappa values ≥ 0.81 indicate strong consistency, 0.61–0.80 indicate good consistency, 0.41–0.60 indicate moderate consistency, 0.21–0.40 indicate fair consistency, and ≤ 0.20 indicate poor consistency. A P value < 0.05 was considered statistically significant.

Results

Patients characteristics and radiation dose

As shown in Fig. 1, we initially prospectively enrolled 160 patients to undergo LE-CTA. After excluding 25 patients, a total of 135 patients were included in Groups A, B, and C, with 45 patients in each group (Fig. 1). There were no statistically significant differences among the groups in terms of gender, age, BMI, comorbidities, coronary artery disease, or surgical history ($P > 0.05$). The scan length showed no statistical differences among the groups. Group A had the highest DLP, ED and contrast dose among three groups ($P < 0.05$), with no statistical differences between Group B and Group C in DLP, ED ($P > 0.05$), while Group B had significantly higher contrast dose than Group C ($P < 0.05$) (Table 1).

Objective image quality

Regarding CT values, Group B showed the highest values at the abdominal aorta and deep femoral artery, followed by Group C, while Group A had the lowest ($P < 0.05$); for the anterior tibial, posterior tibial, fibular, and dorsalis pedis arteries, Group C had the highest values, Group B was next, and Group A had the lowest ($P < 0.05$).

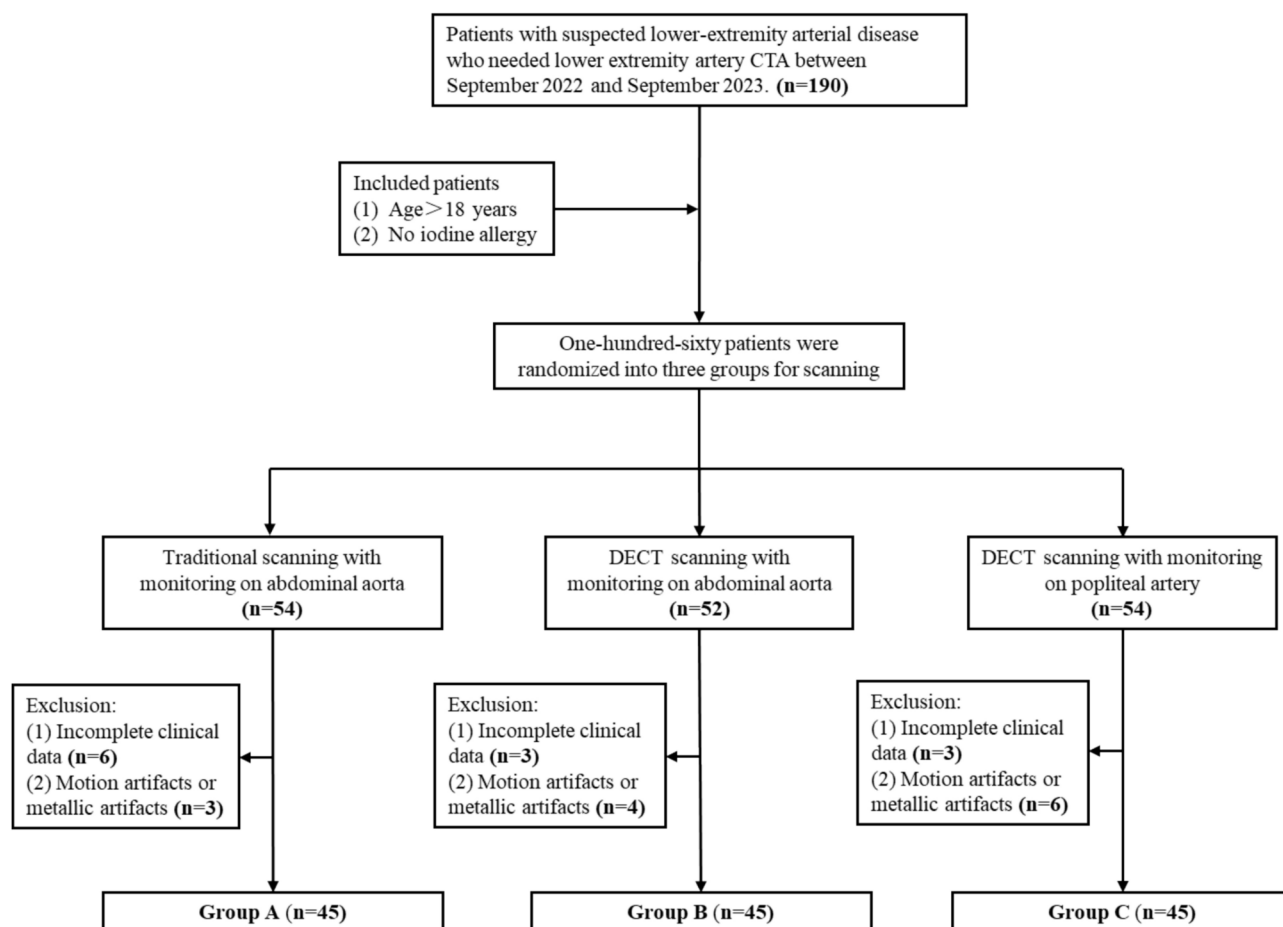


Fig. 1. Flowchart showing the inclusion and exclusion of patients.

	Group A (n = 45)	Group B (n = 45)	Group C (n = 45)	Statistics	P value
Male/female, n	26/19	27/18	30/15	0.56	0.75
Age, years	54.40 ± 15.09	57.51 ± 12.74	57.33 ± 12.51	0.47	0.47
BMI, kg/m ²	23.65 ± 2.82	23.96 ± 3.45	23.27 ± 2.50	0.61	0.54
Underlying disease and surgery					
Diabetes	21	28	25	2.21	0.33
Hypertension	35	29	30	2.17	0.33
Coronary disease	12	9	15	2.04	0.36
Surgery	4	3	3	0.21	0.89
Others	5	4	5	0.15	0.92
Scan length, cm	1171.82 ± 63.02	1189.91 ± 70.90	1195.98 ± 61.50	1.66	0.19
DLP, mGy* cm	653.00 ± 34.01	591.43 ± 31.65	595.83 ± 28.52	53.85	< 0.001 ^{ab}
ED, mSv	4.04 ± 0.34	3.60 ± 0.34	3.53 ± 0.29	31.88	< 0.001 ^{ab}
Contrast medium, mL	105	95	85	134	< 0.001 ^{abc}

Table 1. Patient characteristics and CT scan-related dosages. *BMI body mass index, DLP dose-length product, ED effective dose. ^a $P < 0.05$ for comparison of groups A and B. ^b $P < 0.05$ for comparison of groups A and C. ^c $P < 0.05$ for comparison of groups B and C.

At the popliteal artery, there were no statistical differences between Groups B and C, both of which were higher than Group A ($P < 0.05$). In terms of the noise (SD) values of the seven measured arteries, there was no statistical differences between Groups B and C, both being higher than Group A ($P < 0.05$).

For the signal-to-noise ratio (SNR), Group C had lower values than Groups A and B at the abdominal aorta ($P < 0.05$) and lower values than Group A at the deep femoral artery ($P < 0.05$). At the popliteal artery, Group A had the highest SNR, followed by Group B and then Group C, but the differences were not statistically significant ($P > 0.05$). For the anterior tibial, posterior tibial, fibular, and dorsalis pedis arteries, Group C had the highest SNR, followed by Group B and then Group A ($P < 0.05$).

For the contrast-to-noise ratio (CNR), there were no statistical differences between Groups A and C at the abdominal aorta and deep femoral artery, both being lower than Group B ($P < 0.05$). At the popliteal artery, Group A was lower than Groups B and C ($P < 0.05$). For the anterior tibial, posterior tibial, fibular, and dorsalis pedis arteries, Group C was higher than Groups A and B ($P < 0.05$), with a significant difference only observed at the posterior tibial artery ($P < 0.05$).

Compared to Group B, Group C showed higher SNR and CNR elevation rates (relative to Group A) for arteries more distal than the popliteal artery. For arteries more proximal than the popliteal artery, Group B had higher SNR and CNR elevation rates than Group C. The elevation rates for SNR and CNR in Group C compared to Group B were greater than 0 for arteries more distal than the popliteal artery, while they were less than 0 for more proximal arteries (Table 2, Fig. 2).

Subjective image evaluation

The two physicians demonstrated good to strong consistency in assessing overall image quality and grading of visible below-knee branches, with Kappa values ranging from 0.656 to 0.965. All three groups had overall image quality scores of ≥ 3 , meeting diagnostic requirements.

In the AIS, the subjective scores for the three groups were comparable, with no statistical differences ($P > 0.05$). However, the FPS subjective score for Group A was lower than that of Groups B and C ($P < 0.05$), while there were no statistical differences between Groups B and C ($P > 0.05$). Group C had a significantly higher subjective score for the LKS compared to Groups A and B, and Group B's score was also higher than that of Group A, with both differences being statistically significant ($P < 0.05$). For the grading of below-knee visible branches, Group C's scores were higher than those of Groups A and B ($P < 0.05$), but there were no statistical differences between Groups A and B ($P > 0.05$) (Fig. 3).

Diagnostic consistency and confidence

The diagnostic confidence scores for AIS and FPS from the two physicians showed no statistical differences among the different groups ($P > 0.05$). However, Group C had significantly stronger diagnostic confidence for LKS compared to Groups A and B, and Group B's confidence was also higher than that of Group A, both showing statistical significance ($P < 0.05$), (Table 3, Fig. 3). Figures 4, 5, 6 respectively display the images of three patients obtained through conventional scanning, low-dose DECT with abdominal aorta monitoring, and low-dose DECT with popliteal artery monitoring.

The senior and junior physicians demonstrated strong consistency in diagnosing LE-PAD for AIS and FPS across the three groups, with Kappa values ranging from 0.906 to 1.000. For LKS diagnosis, Group C showed strong consistency (Kappa = 0.956), Group B had good consistency (Kappa = 0.780), while Group A's consistency was lower (Kappa = 0.687), (Table 4).

		Group A (n = 45)	Group B (n = 45)	Group C (n = 45)	Statistics	P value
CT value (HU)	AA	470.04 ± 80.27	847.63 ± 193.86	657.40 ± 196.04	59.79	< 0.001 ^{abc}
	CFA	455.64 ± 74.71	848.27 ± 178.47	696.93 ± 193.16	65.20	< 0.001 ^{abc}
	PA	439.39 ± 72.86	812.85 ± 152.79	783.33 ± 172.04	82.76	< 0.001 ^{ab}
	ATA	366.28 ± 79.01	491.73 ± 75.49	606.46 ± 115.81	66.51	< 0.001 ^{abc}
	PTA	359.68 ± 50.35	489.97 ± 59.04	605.35 ± 111.67	75.79	< 0.001 ^{abc}
	FA	342.67 ± 29.72	452.24 ± 63.92	550.79 ± 94.36	70.40	< 0.001 ^{abc}
	DPA	317.95 ± 43.01	446.85 ± 81.71	538.03 ± 88.40	48.41	< 0.001 ^{abc}
SD (HU)	AA	13.04 ± 2.50	23.18 ± 5.01	24.19 ± 7.13	81.92	< 0.001 ^{ab}
	CFA	12.76 ± 2.80	22.47 ± 6.04	23.41 ± 8.31	73.47	< 0.001 ^{ab}
	PA	7.94 ± 2.46	19.23 ± 6.20	20.33 ± 7.83	59.31	< 0.001 ^{ab}
	ATA	23.63 ± 4.49	31.06 ± 8.34	29.23 ± 8.34	21.33	< 0.001 ^{ab}
	PTA	24.13 ± 5.31	31.44 ± 7.17	28.28 ± 6.15	19.13	< 0.001 ^{ab}
	FA	27.74 ± 8.55	36.64 ± 10.77	31.76 ± 8.97	12.44	0.002 ^{ab}
	DPA	24.50 ± 4.96	32.47 ± 8.15	31.13 ± 6.56	11.63	0.003 ^{ab}
SNR	AA	37.01 ± 9.93	39.63 ± 12.92	28.28 ± 8.69	23.83	< 0.001 ^{bc}
	CFA	36.75 ± 8.61	39.34 ± 12.51	31.47 ± 9.03	10.57	0.005 ^b
	PA	40.34 ± 13.95	43.45 ± 12.37	43.11 ± 16.34	0.59	0.744
	ATA	15.87 ± 4.29	16.99 ± 5.75	22.01 ± 6.05	26.22	< 0.001 ^{bc}
	PTA	15.04 ± 3.82	17.63 ± 5.73	22.52 ± 7.10	28.34	< 0.001 ^{bc}
	FA	13.56 ± 4.57	14.94 ± 5.35	19.04 ± 7.23	16.80	< 0.001 ^{bc}
	DPA	13.48 ± 3.22	14.89 ± 3.94	18.23 ± 5.61	13.38	0.001 ^{bc}
CNR	AA	27.82 ± 11.25	40.93 ± 13.32	30.25 ± 11.77	25.50	< 0.001 ^{ac}
	CFA	27.14 ± 13.8	38.96 ± 12.65	32.09 ± 12.95	22.33	< 0.001 ^{ac}
	PA	23.39 ± 9.71	36.67 ± 10.98	36.79 ± 11.66	41.22	< 0.001 ^{ab}
	ATA	18.44 ± 6.89	20.97 ± 6.12	27.26 ± 7.85	26.53	< 0.001 ^{bc}
	PTA	18.04 ± 8.23	21.03 ± 4.74	27.24 ± 8.62	31.23	< 0.001 ^{abc}
	FA	17.50 ± 7.19	19.99 ± 6.65	24.04 ± 6.38	21.92	< 0.001 ^{bc}
	DPA	16.60 ± 3.76	18.95 ± 5.96	23.62 ± 6.57	15.80	< 0.001 ^{bc}

Table 2. Comparison of quantitative indexes of different groups. AA abdominal aorta, CFA common femoral artery, PA popliteal artery, ATA anterior tibial artery, PTA posterior tibial artery, FA fibular artery, DPA dorsalis pedis artery, SNR signal-to-noise ratio, CNR contrast-to-noise ratio. ^a*P* < 0.05 for comparison of groups A and B. ^b*P* < 0.05 for comparison of groups A and C. ^c*P* < 0.05 for comparison of groups B and C. Data in mean ± standard deviation.

Discussion

This study explored the artery depiction and diagnostic performance using DECTs and the popliteal artery monitoring in threshold triggering LE-CTA scanning with a dual-low dose protocol. Compared to the conventional scanning, the dual-low dose protocol combining DECTs with popliteal artery monitoring provides excellent delineation of distal end of lower-extremity arteries, with particularly notable improvements for below-knee artery display, under reductions in radiation dose and contrast agent volume by 12.62% and 19.0%, respectively.

The improvement in visualization of the lower-extremity arteries was supported by both DECTs and monitoring site optimization. Notably, DECTs improved the iodine enhancement, thus promoted the visibility of all seven lower extremity arteries, with the SNR and CNR elevation rates of Group-B exceeding zero (elevation_{B to A}). Previous studies^{7,9} also showed enhanced iodine contrast and ameliorated visibility of lower extremity arteries on lower-keV monoenergetic images, accordant with our findings. Furthermore, our study demonstrated better results with less contrast and radiation dose. However, this extensive improvement in artery visibility only results in the enhancement of subjective image scores, diagnostic confidence, and diagnostic consistency for LKS, but not other segments. This may be attributed to the smaller lumen diameters and greater flow resistance in the distal arteries, which limited the contrast enhancement, while the proximal arteries with larger diameters already provided high diagnostic confidence in conventional scanning, leading to no statistically significant differences among groups.

The popliteal artery monitoring-triggered scanning specifically enhanced the display of arteries more distal than the popliteal artery. With 10 mL of contrast reduced, the SNR and CNR of below-knee arteries in images with DECTs combining PA monitoring were increased by 18.32–22.80% and 16.84–23.07% (elevation_{C to B}), respectively; while those of more proximal arteries (AA, CFA) were inferior compared to DECTs with AA monitoring. In the LKS, the visibility of small vascular branches and diagnostic confidence, as well as consistency between junior and senior physicians were also significantly improved by PA monitoring. It is notable that at the optimized monitoring point (popliteal artery), SNR and CNR were comparable between AA monitoring

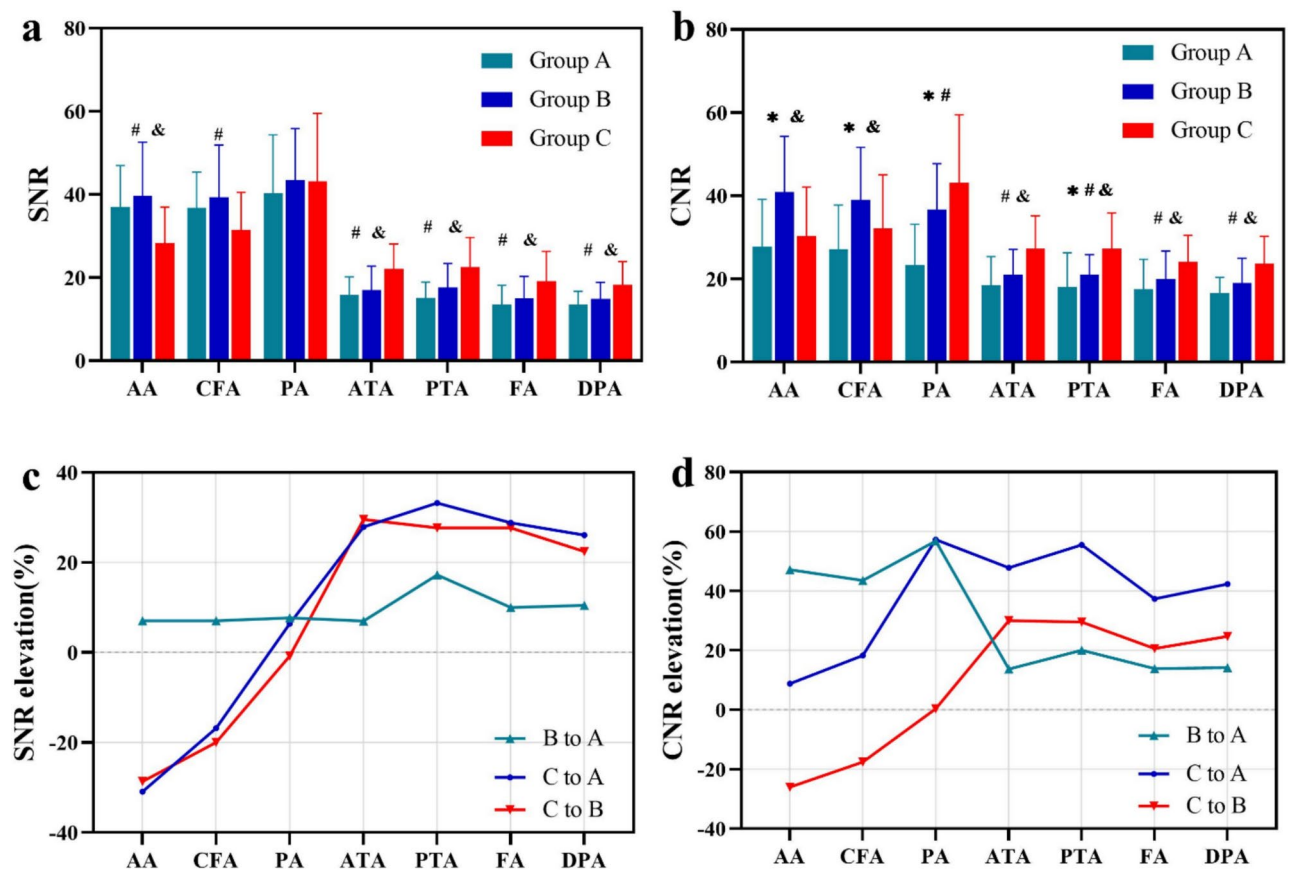


Fig. 2. Comparison of quantitative indexes of different groups (a) shows the comparison of SNR values of three groups at different ROI. (b) Shows the comparison of CNR values of three groups at different ROI. (c) Shows the SNR elevation of group B and group C at different ROI. (d) Shows the CNR elevation of group B and group C at different ROI. AA: abdominal aorta, CFA: common femoral artery, PA: popliteal artery; ATA: anterior tibial artery, PTA: posterior tibial artery, FA: fibular artery, DPA: dorsalis pedis artery; SNR, signal-to-noise ratio; CNR, contrast-to-noise ratio; * $P < 0.05$ for comparison of groups A and B; # $P < 0.05$ for comparison of groups A and C; & $P < 0.05$ for comparison of groups B and C.

and PA monitoring groups. Thus, we speculate that shifting the monitoring point to the distal location improves visibility for more distal arteries but may not benefit proximal arteries as effectively as AA monitoring. This is attributed to the PA monitoring threshold-triggered scan, which optimizes the scanning time only according to the peak enhancement of the LKS. In Group C, the scan was initiated with an 8-s delay after the PA's CT attenuation reached the threshold. This led to a scanning phase that more close to the peak enhancement time of the below-knee arteries, while creating a delay in the peak enhancement time of the proximal abdominal aorta and femoral artery. Differences in CT attenuation for the same arteries scanned with different monitoring sites resulted in distinct variations in SNR and CNR between the below-knee and above-knee arteries in Groups B and C. Notably, the lower contrast agent volume used in Group C also weakened SNR and CNR performance across all arteries. Previous studies using ankle artery monitoring for LCTA scans with foot-to-head direction did not perform comparative analyses²³. Additionally, David et al.¹⁸ found that traditional scanning at foot-to-head directions with popliteal artery monitoring did not enhance overall lower extremity vessel visibility. While this scanning method may be useful for obstructive diseases in below-knee arteries, it was less effective for depicting proximal arteries, which is accordant to our results. Therefore, under the dual low-dose conditions (lower radiation and contrast agent volumes), DECTs is required when optimizing the monitoring point to the popliteal artery, to ensure adequate contrast for proximal arteries and enable excellent visualization of both proximal and distal arteries (median subjective image scores of 5) and high diagnostic efficacy (with diagnostic consistency for Group C ranging from 0.906 to 0.956). Notably, Although DECT improves CNR in the AIS to levels comparable to or exceeding conventional scanning, SNR remains suboptimal. Therefore, the choice of monitoring site should be tailored to clinical priorities—if proximal artery assessment is crucial, AA monitoring may still be preferred.

In our study, patients ultimately received a radiation exposure of 3.53 ± 0.29 mSv and 85 mL of contrast agent (350 mgI/mL), representing reductions of 12.62% and 19.0%, respectively, compared to the conventional group. The radiation dose in this study is slightly lower than that reported in other studies utilizing DECTs with similar devices (3.80 ± 0.80 mSv)⁹. While the amount of contrast agent used in our study is not as low as in

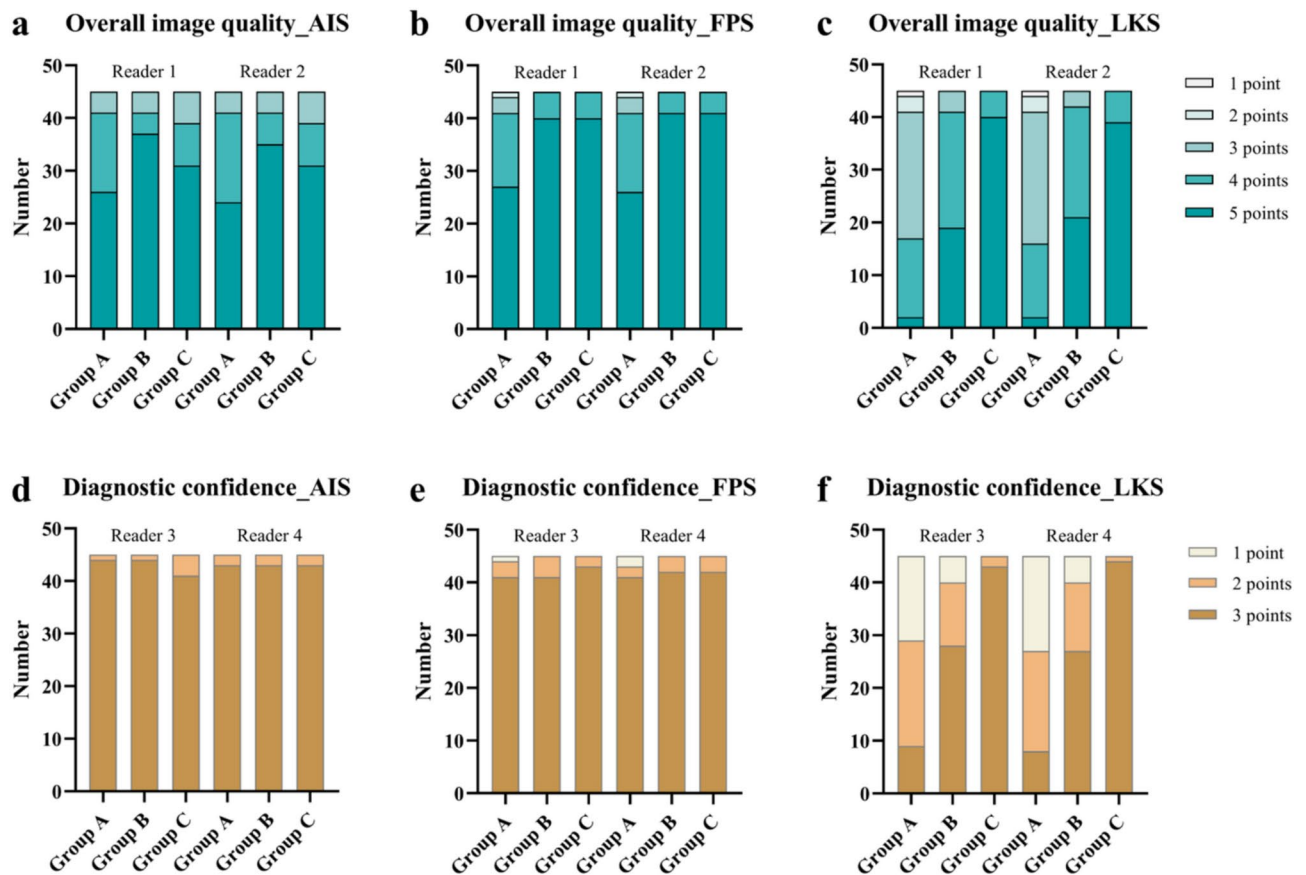


Fig. 3. Comparison of subjective image quality and diagnosis confidence of three groups in different segments. AIS: Abdominal Iliac Segment; FPS: Femoral Popliteal Segment; LKS: Lower Knee Segment.

some previous literature (55.4 mL and 45 mL), those studies primarily utilized dual-layer detector DECTs, with effective radiation doses for patients being $9.58 (1.36) \text{ mSv}^{17}$ and $11.88 \pm 2.67 \text{ mSv}^{19}$, significantly higher than in our research. Of course, other techniques such as low kVp combined with deep learning image reconstruction algorithms^{24,25} and high pitch scanning can also reduce radiation doses^{26,27}. Our study utilized 50 keV images because, at lower radiation doses, although iodine CT values are higher at 40 keV, the noise level is intolerable. Reducing noise in 40 keV images through advanced reconstruction algorithms may further decrease the required amount of iodinated contrast agent. This would be particularly beneficial in minimizing the risk of radiation-induced cancer and contrast-induced nephropathy, especially for patients with renal impairment. Notably, compared to a conventional scanning mode, the single-source fast-switching DECTs our study used not only provides monoenergetic images but also material density maps (iodine maps²⁸, muscle maps²⁹, etc.), which may offer additional clinical value for assessing vascular diseases and the severity of ischemic involvement in muscle, warranting further investigation.

This study also has some limitations: (1) single-center study may introduce bias; (2) the included cases did not focus on specific disease types, nor did we obtain DSA results as a diagnosis reference; (3) personalized contrast agent protocols based on patient weight were not implemented; (4) Patients with impaired renal function were not included. Moreover, reducing electronic noise in lower keV images through advanced reconstruction algorithms may further decrease the required contrast agent dosage, a low contrast dose protocol is particularly significant for them; (5) comparisons of image quality with monitoring points in other regions (e.g., thigh, calf, foot) have not been investigated. These aspects will be addressed in future research.

In summary, DECTs with PA monitoring offers outstanding display of lower-extremity arteries under dual low-dose conditions, especially improving the LKS. This approach not only boosts diagnostic confidence but also improves consistency in diagnoses between radiologists with varying levels of experience, highlighting its significant potential for PAD diagnosis particularly for those located at LKS.

		Group A (n = 45)	Group B (n = 45)	Group C (n = 45)	Statistics	P value
Subjective image quality						
AIS* score	Reader 1	5 (3.5)	5 (3.5)	5 (3.5)	4.99	0.082
	Reader 2	5 (3.5)	5 (3.5)	5 (3.5)	4.68	0.096
Kappa		0.933	0.908	0.927		
FPS* score	Reader 1	5 (2.5)	5 (4.5)	5 (4.5)	17.71	< 0.001 ^{ab}
	Reader 2	5 (2.5)	5 (4.5)	5 (4.5)	19.79	< 0.001 ^{ab}
Kappa		0.775	0.726	0.895		
LKS* score	Reader 1	3 (1.5)	4 (3.5)	5 (4.5)	76.15	< 0.001 ^{abc}
	Reader 2	3 (1.5)	4 (3.5)	5 (4.5)	76.2	< 0.001 ^{abc}
Kappa		0.897	0.896	0.911		
LKS*Vascular grading	Reader 1	3 (1.5)	4 (1.5)	5 (3.5)	45.73	< 0.001 ^{bc}
	Reader 2	3 (1.5)	4 (1.5)	5 (3.5)	46.81	< 0.001 ^{bc}
Kappa		0.962	0.952	0.965		
Diagnostic confidence						
AIS*score	Reader 3	3 (2.3)	3 (2.3)	3 (2.3)	0.51	0.774
	Reader 4	3 (2.3)	3 (2.3)	3 (2.3)	0.29	0.861
Kappa		0.656	0.656	0.789		
FPS* score	Reader 3	3 (1.3)	3 (2.3)	3 (2.3)	2.14	0.334
	Reader 4	3 (1.3)	3 (2.3)	3 (2.3)	0.78	0.675
Kappa		0.902	0.656	0.845		
LKS* score	Reader 3	2 (1.3)	3 (1.3)	3 (2.3)	51.24	< 0.001 ^{abc}
	Reader 4	2 (1.3)	3 (1.3)	3 (2.3)	56.46	< 0.001 ^{abc}
Kappa		0.942	0.967	0.789		

Table 3. Comparison of subjective evaluation of image quality, diagnostic confidence, and grading of infrapopliteal vessels in three groups. *AIS abdominal iliac segment, FPS femoral popliteal segment, LKS lower knee segment. ^a $P < 0.05$ for comparison of groups A and B. ^b $P < 0.05$ for comparison of groups A and C. ^c $P < 0.05$ for comparison of groups B and C. Data in median (minimum, maximum).

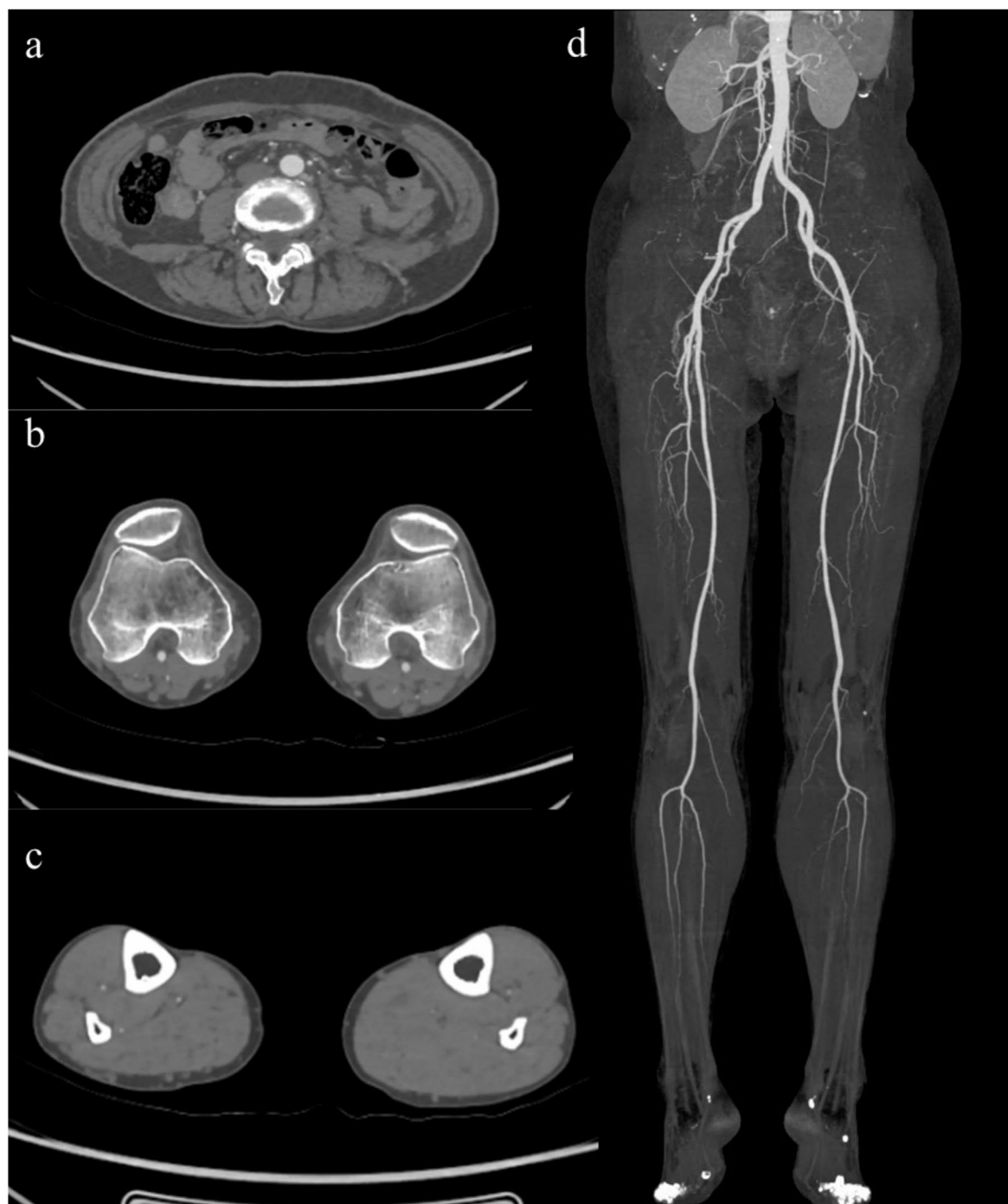


Fig. 4. A 70-year-old male patient with a history of smoking and intermittent claudication in the right lower limb underwent routine lower limb artery CTA (abdominal aorta monitoring). (a) Show abdominal liliac segment. (b) Show femoral popliteal segment. (c) Show lower knee segment. (d) Show maximum intensity projection of peripheral arteries. The overall image quality was moderate, with insufficient contrast enhancement in the LKS region. A senior physician diagnosed no significant abnormalities in the lower limb arteries, while the junior physician had low confidence in the LKS diagnosis. Subjective scores were AIS: 4, FPS: 3, LKS: 3, with a lower limb vessel grading of 2. Diagnostic confidence levels were AIS: 3, FPS: 3, LKS: 1.



Fig. 5. A 64-year-old female patient with hypertension underwent lower extremity DE-CTA (with abdominal aorta monitoring) due to leg pain. **(a)** Show abdominal iliac segment. **(b)** Show femoral popliteal segment. **(c)** Show lower knee segment. **(d)** Show maximum intensity projection of peripheral arteries. The image quality was good with significant contrast enhancement, though the visualization of below-knee arteries was faint. The senior physician diagnosed no significant abnormalities in the lower extremity arteries, but the junior physician expressed low confidence in diagnosing the LKS region. Subjective scores were AIS: 5, FPS: 4, LKS: 4; with a below-knee arterial grading of 3. Diagnostic confidence levels were AIS: 3, FPS: 3, LKS: 2.



Fig. 6. A 51-year-old male patient with diabetes and intermittent right lower limb pain underwent DE-CTA of the lower limb arteries with popliteal artery monitoring. **(a)** Show abdominal iliac segment. **(b)** Show femoral popliteal segment. **(c)** Show lower knee segment. **(d)** Show maximum intensity projection of peripheral arteries. The image quality was excellent, with significantly enhanced contrast and clear visualization of the vessels below the knee. Both physicians diagnosed severe stenosis and occlusion of the right posterior tibial artery as indicated by the arrow. The subjective scores were AIS: 5, FPS: 5, LKS: 5, with a lower limb vessel grading of 5. The diagnostic confidence levels were AIS: 3, FPS: 3, LKS: 3.

	Group A		Group B		Group C	
	Senior	Junior	Senior	Junior	Senior	Junior
AIS						
Positive	48.88% (22/45)	48.88% (22/45)	55.55% (25/45)	55.55% (25/45)	68.88% (31/45)	68.88% (31/45)
Kappa	1.000		1.000		1.000	
FPS						
Positive	33.33% (14/45)	31.11% (15/45)	26.66% (11/45)	24.44% (13/45)	40.00% (18/45)	35.55% (16/45)
Kappa	0.947		0.942		0.906	
LKS						
Positive	48.88% (22/45)	33.33% (15/45)	55.55% (25/45)	44.44% (20/45)	51.11% (23/45)	48.88% (22/45)
Kappa	0.687		0.780		0.956	

Table 4. Comparison of lesion detection about senior and junior doctors of three groups. AIS abdominal iliac segment, FPS femoral popliteal segment, LKS lower knee segment. Positive data in % and number.

Data availability

Data is provided within the manuscript.

Received: 7 December 2024; Accepted: 8 April 2025
Published online: 09 May 2025

References

1. Firnhaber, J. M. & Powell, C. S. Lower extremity peripheral artery disease: Diagnosis and treatment. *Am. Fam. Physician* **99**, 362–369 (2019).

2. Hiatt, W. R. et al. Atherosclerotic peripheral vascular disease symposium II: Nomenclature for vascular diseases. *Circulation* **118**, 2826–2829 (2008).

3. Lin, J., Chen, Y., Jiang, N., Li, Z. & Xu, S. Burden of peripheral artery disease and its attributable risk factors in 204 countries and territories from 1990 to 2019. *Front. Cardiovasc. Med.* **9**, 868370 (2022).

4. Fowkes, F. G. et al. Comparison of global estimates of prevalence and risk factors for peripheral artery disease in 2000 and 2010: A systematic review and analysis. *Lancet* **382**, 1329–1340 (2013).

5. Shwaiki, O. et al. Lower extremity CT angiography in peripheral arterial disease: From the established approach to evolving technical developments. *Int. J. Cardiovasc. Imaging* **37**, 3101–3114 (2021).

6. Foley, W. D. & Stonely, T. CT angiography of the lower extremities. *Radiol. Clin. N. Am.* **48**, 367–396 (2010).

7. Wichmann, J. L. et al. Dual-energy computed tomography angiography of the lower extremity runoff: Impact of noise-optimized virtual monochromatic imaging on image quality and diagnostic accuracy. *Invest. Radiol.* **51**, 139–146 (2016).

8. Mishra, A., Jain, N. & Bhagwat, A. CT angiography of peripheral arterial disease by 256-slice scanner: Accuracy, advantages and disadvantages compared to digital subtraction angiography. *Vasc. Endovasc. Surg.* **51**, 247–254 (2017).

9. Jia, X. et al. Improving diagnostic accuracy for arteries of lower extremities with dual-energy spectral CT imaging. *Eur. J. Radiol.* **128**, 109061 (2020).

10. Gruschwitz, P. et al. Noise-optimized virtual monoenergetic reconstructions of dual-energy CT angiographies improve assessability of the lower leg arterial segments in peripheral arterial occlusive disease. *Radiography* **29**, 19–27 (2023).

11. Scheschenja, M. et al. CT angiography of the lower limbs: Combining small field of view with large matrix size and iterative reconstruction further improves image quality of below-the-knee arteries. *Acta Radiol.* **65**, 774–783 (2024).

12. Sommer, W. H. et al. Diagnostic value of time-resolved CT angiography for the lower leg. *Eur. Radiol.* **20**, 2876–2881 (2010).

13. Buls, N. et al. Improving the diagnosis of peripheral arterial disease in below-the-knee arteries by adding time-resolved CT scan series to conventional run-off CT angiography. First experience with a 256-slice CT scanner. *Eur. J. Radiol.* **110**, 136–141 (2019).

14. Matsumoto, K. et al. Virtual monochromatic spectral imaging with fast kilovoltage switching: Improved image quality as compared with that obtained with conventional 120-KVp CT. *Radiology* **259**, 257–262 (2011).

15. Bucolo, G. M. et al. Virtual monoenergetic imaging of lower extremities using dual-energy CT angiography in patients with diabetes mellitus. *Diagnostics* **13**, 1790 (2023).

16. Kim, J. S. et al. Imaging findings of peripheral arterial disease on lower-extremity CT angiography using a virtual monoenergetic imaging algorithm. *J. Korean Soc. Radiol.* **83**, 1032–1045 (2022).

17. Kristiansen, C. H. et al. Halved contrast medium dose in lower limb dual-energy computed tomography angiography: A randomized controlled trial. *Eur. Radiol.* **33**, 6033–6044 (2023).

18. Rotzinger, D. C. et al. Computed tomography angiography in peripheral arterial disease: Comparison of three image acquisition techniques to optimize vascular enhancement-randomized controlled trial. *Front. Cardiovasc. Med.* **7**, 68 (2020).

19. Ren, H. et al. Feasibility of low-dose contrast media in run-off CT angiography on dual-layer spectral detector CT. *Quant. Imaging Med. Surg.* **11**, 1796–1804 (2021).

20. Hamady, M. & Muller-Hulsbeck, S. European society for vascular surgery (ESVS) 2020 clinical practice guidelines on the management of acute limb ischaemia; A word of caution!. *CVIR Endovasc.* **3**, 31 (2020).

21. Meyer, B. C. et al. Do the cardiovascular risk profile and the degree of arterial wall calcification influence the performance of MDCT angiography of lower extremity arteries?. *Eur. Radiol.* **20**, 497–505 (2010).

22. Bai, Y. et al. MRI: Evaluating the application of FOCUS-MUSE diffusion-weighted imaging in the pancreas in comparison with FOCUS, MUSE, and single-shot DWIs. *J. Magn. Reson. Imaging* **57**, 1156–1171 (2023).

23. Chen, Y. et al. The effects of deep learning image reconstruction algorithm on image quality of lower extremity CT angiography with low kV and reverse flow direction scanning. *Chin. J. Radiol.* **56**, 1188–1194 (2022).

24. Li, W. et al. High-strength deep learning image reconstruction in coronary CT angiography at 70-KVp tube voltage significantly improves image quality and reduces both radiation and contrast doses. *Eur. Radiol.* **32**, 2912–2920 (2022).

25. Noda, Y. et al. Comparison of image quality and pancreatic ductal adenocarcinoma conspicuity between the low-KVp and dual-energy ct reconstructed with deep-learning image reconstruction algorithm. *Eur. J. Radiol.* **159**, 110685 (2023).

26. Kravchenko, D. et al. Image quality and radiation dose of dual source high pitch computed tomography in pediatric congenital heart disease. *Sci. Rep.* **12**, 9934 (2022).

27. Ma, Y. et al. Feasibility study of using low-kilovoltage, prospective gating, high-pitch, dual-source computed tomography prior to transcatheter aortic valve replacement: Analysis of image quality and radiation dose. *J. Thorac. Dis.* **15**, 6848–6857 (2023).
28. Liang, H. et al. Dual-energy CT with virtual monoenergetic images and iodine maps improves tumor conspicuity in patients with pancreatic ductal adenocarcinoma. *Insights Imaging* **13**, 153 (2022).
29. Liu, Y. Y. et al. Diagnostic value of dual-energy CT and clinicopathological and imaging feature analysis of mixed endometrial stromal and smooth muscle tumors with intracardiac extension. *Front. Cardiovasc. Med.* **9**, 917399 (2022).

Acknowledgements

This study has received funding by the Natural Science Foundation of Hubei Province (Grant Number: 2023AFC033).

Author contributions

W.C.M., C.L., W.C. (Guarantors of integrity of entire study); all authors (study concepts/study design or data acquisition or data analysis/interpretation); W.C.M., C.L., W.C. (manuscript drafting or manuscript revision for important intellectual content); all authors (approval of final version of submitted manuscript); all authors (agrees to ensure any questions related to the work are appropriately resolved); W.C.M., Q.T., C.C.L., S.W., (literature research); Q.Q.Z., S.P.C., W.C. (clinical studies); L.X.; W.C. (experimental studies); W.C.M., C.L., Q.T., S.P.C., W.C. (statistical analysis); W.C.M., Q.T. (and manuscript editing).

Declarations

Competing interests

The authors declare no competing interests.

Additional information

Correspondence and requests for materials should be addressed to C.L. or W.C.

Reprints and permissions information is available at www.nature.com/reprints.

Publisher's note Springer Nature remains neutral with regard to jurisdictional claims in published maps and institutional affiliations.

Open Access This article is licensed under a Creative Commons Attribution-NonCommercial-NoDerivatives 4.0 International License, which permits any non-commercial use, sharing, distribution and reproduction in any medium or format, as long as you give appropriate credit to the original author(s) and the source, provide a link to the Creative Commons licence, and indicate if you modified the licensed material. You do not have permission under this licence to share adapted material derived from this article or parts of it. The images or other third party material in this article are included in the article's Creative Commons licence, unless indicated otherwise in a credit line to the material. If material is not included in the article's Creative Commons licence and your intended use is not permitted by statutory regulation or exceeds the permitted use, you will need to obtain permission directly from the copyright holder. To view a copy of this licence, visit <http://creativecommons.org/licenses/by-nc-nd/4.0/>.

© The Author(s) 2025